

Microtomography: Polymer Blends, Atherosclerosis, and Comparison of Instrumentation

L. G. Butler,¹ K. Ham,² H. Jin,³ R. L. Kurtz,³ M. Rivers⁴

¹Department of Chemistry, ²Center for Advanced Microstructures & Devices (CAMD), and

³Department of Physics and Astronomy, Louisiana State University (LSU), Baton Rouge, LA, U.S.A.

⁴GeoSoilEnviro Consortium for Advanced Radiation Sources (GSECARS), The University of Chicago, Chicago, IL, U.S.A.

Introduction

Consider the plastic shell of a typical cathode ray tube (CRT) monitor. Did you know that up to 30% (by mass) is bromine? Then consider the calcifications attached to arterial walls. New calcifications can develop within a few years after a heart bypass operation. These samples and more were imaged at the APS GSECARS and LSU CAMD tomographic beamlines, and ideas were shared about the acquisition and analysis of tomographic data.

Methods and Materials

Flame Retardants

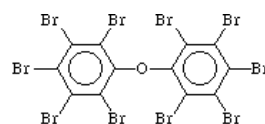
Three issues are associated with brominated aromatic flame retardants. First, the solubility of the brominated aromatic with high-impact polystyrene (HIPS) varies, depending on the molecular structure of the brominated aromatic. Good miscibility is desired, or else the stability of the final product can be poor. Second, brominated aromatics are difficult to observe with some of the more common spectroscopic methods typically used for polymer blend characterization. For example, solid-state ¹³C nuclear magnetic resonance (NMR) is a common spectroscopic method for polymer studies, yet the quadrupolar bromine nucleus causes such line broadening of the ¹³C resonances that miscibility is difficult to ascertain from the spectrum; hence, the relatively uncommon technique of ⁸¹BR nonmagnetic quadrupole resonance (NQR) is used [1]. Third, there is some concern about the bioaccumulation of brominated aromatics, especially phenolic degradation products of perbrominated biphenyl ethers, and their subsequent role as estrogen mimics [2]. Commercial brominated flame retardants (Fig. 1) have different solubilities in HIPS. An aromatic ether — 1-(2,3,4,5,6-pentabromophenoxy)-2,3,4,5,6-pentabromobenzene (Saytex 102) — is miscible in HIPS. However, a somewhat larger molecule — 3,3',4,4',5,5',6,6' -octabromo-N,N' -ethylenedipthalimide (Saytex BT-93), appears to exist as microcrystalline domains dispersed in HIPS. Although in principle, NMR imaging could be used to study miscibility, we consider synchrotron radiation microtomography to be a faster and more informative technique.

Atherosclerosis

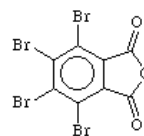
Human atherosclerotic arteries removed from three white males aged 51, 55, and 70 years old were measured. The arteries were obtained from the Pathology Department of the LSU Medical Center in New Orleans. Two kinds of arteries, native and bypass, were used in this study. Images of each native artery were taken at two different heights. Figure 2 is a schematic drawing of a native and a bypass artery. Native arteries were present since birth, and bypass arteries were inserted during heart bypass surgery. The bypass arteries were removed because they filled up again with plaque. The native arteries of the A and B specimens were from the left circumflex. The C sample was from the anterior descending coronary artery. Each artery was cut to be about 20 mm long and inserted longitudinally into a plastic straw. Each sample was packed in a separate straw, and each straw was sealed at the bottom and top to prevent dehydration. The arteries were kept frozen before the tomographic measurements. Experiments were done after the arteries thawed.

Tomography at the LSU CAMD Synchrotron

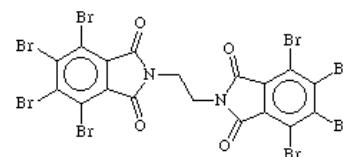
The most significant differences between the two beamlines occur with regard to available x-ray energies,



1-(2,3,4,5,6-pentabromophenoxy)-2,3,4,5,6-pentabromobenzene (Saytex 102)



3,4,5,6-tetrabromophthalic anhydride (Saytex RB-49)



3,3',4,4',5,5',6,6'-octabromo-N,N'-ethylenedipthalimide (Saytex BT-93)

FIG. 1. Brominated aromatic flame retardants.

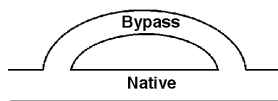


FIG. 2. Schematic drawing of a native artery and bypass.

table motorization, and the fraction of time devoted to tomography. Currently, CAMD tomography is done on a bending magnet that, at a 1.5-GeV ring energy, generates significant flux up to 15 keV. However, we have not yet installed a monochromator, so a filtered white beam is used. The CAMD and APS sample and camera stages employ similar table motorization, but the APS system has a superior table alignment system. The CAMD tomographic instrument is the only one currently installed at this bending magnet; therefore, it offers the opportunity for very long tomographic runs, subject to CAMD ring operations. There are some minor differences between the two systems. The CAMD uses a two-computer system. A Linux computer operates the charge-coupled device, and a Macintosh computer operates the motors. Both computers are programmed with LabVIEW (the LabVIEW TCP/IP routines are useful for fast inter-system communication). Matlab and IDL are used for image processing. Routines have been developed for CCD assessment (hot/cold pixel detection) and tomographic alignment on the basis of the difference imaging of a wire screen (thanks to J. Dunsmuir of Exxon).

Results

Flame Retardants

Tomographic data sets were acquired above and below the Br K edge at 13.47 keV. The multiple 3-D images were converted to a single 3-D map of the distribution of flame retardant by a voxel-by-voxel nonlinear least squares fit of x-ray absorption. The absorptions of the pure phases — flame retardant and HIPS — were calculated from the National Institute of Standards and Technology (NIST) database, and the least squares routine was constrained to return physically reasonable flame retardant concentrations for each voxel. The 3-D flame retardant image (Fig. 3) clearly shows an inhomogeneous distribution of BT-93, the least soluble flame retardant. A preliminary particle size analysis was done.

Atherosclerosis

Three types of plaque components were distinguished by brightness in these samples. They indicated low, medium, and high mass densities, as previously shown by other clinical imaging methods. The low-density component was identified as being fatty plaque (consisting of lipid-rich deposits); the medium-density

component is fibrous plaque; and the high-mass-density particles are calcified plaque [4, 5]. These three phases of particles were observed as indicated by the absorption profile shown in Fig. 4. The absorption coefficient by fibrous plaque of 12.5-keV x-rays is about 2.28 cm^{-1} , twice that of fatty plaque. The calcium deposit has around 10 times higher absorption than the fibrous plaque. The cross-sectional images of the native arteries clearly show the 3-D morphologies and distributions of the plaque components in atherosclerotic arteries. Some calcified plaques were separately distributed as small clusters, while some are large continuous pieces along the vessel axis. The density of the calcification edges was higher

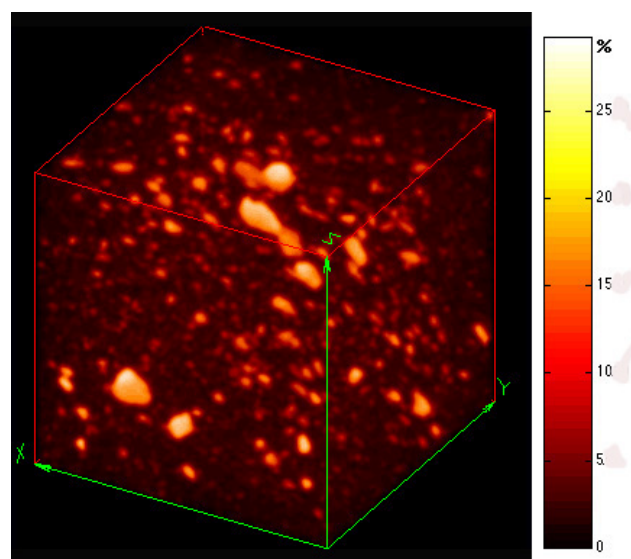


FIG. 3. Three-dimensional image of flame retardant.

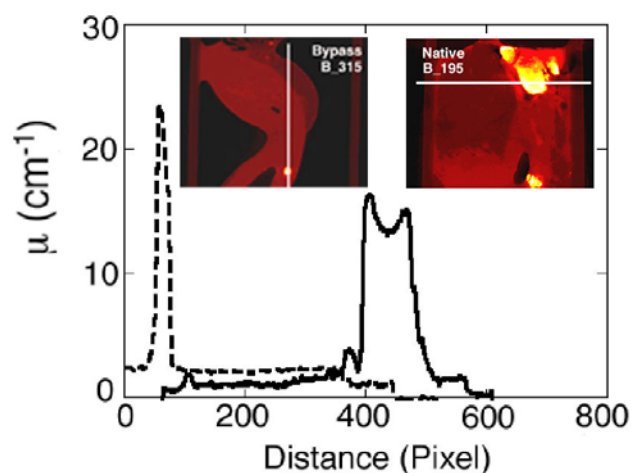


FIG. 4. Absorption along the bypass (dashed line) and native (solid line) arteries of a 55-year-old male. These lines span all three plaque phases and air.

than that of the interiors, which is also shown in Fig. 4. The volume fraction of calcification was determined by thresholding the absorption of calcification and air to estimate volumes of calcified plaques and artery wall. The volume ratios of calcification to artery wall for the three native samples were $3.7 \pm 0.2\%$, $6.0 \pm 1.3\%$, and $20 \pm 3\%$, while the ratios for the bypass specimens were only $0.025 \pm 0.004\%$, $0.032 \pm 0.007\%$, and $0.021 \pm 0.002\%$ — orders of magnitude lower than the ratios for the native samples.

Discussion

Tomography with a filtered white beam is useful for obtaining information about gross structural features. However, more detailed information is available by combining images acquired at multiple x-ray energies.

Acknowledgments

A grant from the Louisiana Board of Regents supported construction of the CAMD tomographic beamline. We thank B. S. Gupta (Department of Geology and Geophysics, LSU) and L. S. Simeral (Albemarle Corp.) for their interesting samples. K. Ham and H. Jin

acknowledge support from CAMD and the LSU Biological Computation and Visualization Center, respectively. Tomographic polymer studies are supported in part by a grant from the Petroleum Research Foundation of the American Chemical Society. Use of the APS was supported by the U.S. Department of Energy, Office of Science, Office of Basic Energy Sciences, under Contract No. W-31-109-ENG-38. We also acknowledge support from the GSECARS Collaborative Access Team (CAT).

References

- [1] A. A. Mrse, Y. Lee, P. L. Bryant, F. R. Fronczek, L. G. Butler, and L. S. Simeral, *Chem. Mater.* **10**, 1291-1300 (1998).
- [2] K. S. Betts, *Environ. Sci. Technol.* **35**, 274A-275A (2001).
- [3] L. G. Butler, K. Ham, H. Jin, and R. L. Kurtz, *SPIE Proc.* **4503** (2001).
- [4] R. A. Vogel, *Am. J. Cardiac Imaging* **2**, 110-115 (1988).
- [5] S. Vallabhajosula and V. Fuster, *J. Nucl. Med.* **38**, 1788-1796 (1997).